

Spin filtering in a hybrid ferromagnetic-semiconductor microstructure

J. Wróbel,^{1,2} T. Dietl,^{1,2} A. Lusakowski,¹ G. Grabecki,^{1,2} K. Fronc,¹ R. Hey,³ K. H. Ploog,³ and H. Shtrikman⁴

¹*Institute of Physics, Polish Academy of Sciences, al. Lotników 32/46, 02-668 Warszawa, Poland*

²*ERATO Semiconductor Spintronics Project, Japan Science and*

Technology Agency, al. Lotników 32/46, 02-668 Warszawa, Poland

³*Paul Drude Institute of Solid State Electronics, Hausvogteiplatz 5-7, D-10117 Berlin, Germany*

⁴*Center for Submicron Research, Weizmann Institute of Science, Rehovot 76100, Israel*

We fabricated a hybrid structure in which cobalt and permalloy micromagnets produce a local in-plane spin-dependent potential barrier for high-mobility electrons at the GaAs/AlGaAs interface. Spin effects are observed in ballistic transport in the tens' millitesla range of the external field, and are attributed to switching between Zeeman and Stern-Gerlach modes – the former dominating at low electron densities.

PACS numbers: 85.75.-d, 72.25.Dc, 73.23.ad

Long spin coherence times in semiconductors have triggered considerable efforts towards developing devices, in which functionalities would involve spin degrees of freedom [1]. An important building block of such devices is a spin-filter, which could serve for either generating or detecting spin-polarized currents and, indeed, spin filtering capabilities of quantum point contacts [2, 3] and quantum dots [4, 5, 6] have recently been demonstrated. In those devices, a spin dependent barrier occurs as a result of the Zeeman spin-splitting generated by a strong uniform *external* magnetic field. Also the Stern-Gerlach (S-G) effect has been theoretically considered as a possible spin-filter in spin-logic processors [7]. There are, however, fundamental arguments against the occurrence of the S-G effect for beams of electrons [11], a problem that attracts persistent attention [12, 13, 14]. At the same time, the progress in fabrication of hybrid ferromagnet-semiconductor microstructures [8, 9] has made it possible to address various aspects of electron transport in the presence of an inhomogeneous magnetic field [10, 15, 16, 17, 18, 19]. For example, the present authors have proposed a way to achieve spin separation by using a Stern-Gerlach apparatus for the conduction electrons residing in a quantum well and exposed to a gradient of the in-plane magnetic field [18].

In this Letter, we report on the effect of a *local* in-plane magnetic field on ballistic currents in a quantum wire patterned of GaAs/GaAlAs heterostructure. The results are obtained for a ferromagnet-semiconductor hybrid device which is highly optimized in order to toggle between Zeeman-like (uniform field) and Stern-Gerlach-like (field gradient) internal spin barriers. By comparing our findings to results of conductance computations by the recursive Green-function method, we find out that the Zeeman effect dominates, particularly at low carrier densities. Owing to spin filtering and detecting capabilities that occur in a weak external magnetic field, our microstructure thus emerges as a perspective component of spintronic devices.

Figure 1(a) presents a micrograph of our device, whose

design results from an elaborated optimization process [18], and whose fabrication involves five electron beam lithography levels, two wet etching steps, and deposition by low-power magnetosputtering and lift off of four different metals. A two-dimensional electron gas (2DEG) resides 95 nm below the top surface of a quantum wire of the geometrical width smoothly increasing from 0.7 to 1.4 μm , chemically etched from a modulation Si-doped (001) GaAs/(Al,Ga)As heterostructure, which was grown in the Drude Institute in Berlin. The wire is patterned along the [110] crystal axis, for which the direction of a fictitious magnetic field brought about by spin-orbit effects will be parallel to the field gradient and, therefore, will weakly affect spin dynamics [22]. The electron mobility prior to nanofabrication is $\mu = 1.76 \times 10^6$ cm^2/Vs in the dark. Hence, with the electron density $n = 2.3 \times 10^{11}$ cm^{-2} , the mean free path is of the order of the channel length. A local magnetic field is produced by NiFe (permalloy, Py) and cobalt (Co) films. The micromagnets of dimensions $40 \times 7 \times 0.1$ μm^3 reside in 0.15 ± 0.05 μm deep groves on the two sides of the wire, so that the 2DEG is approximately at the center of the field. To prevent stripe oxidation and to avoid accumulation of electrostatic charges, both micromagnets are covered with a thin (20 nm) protecting AuPd layer and connected to separate contact pads. Additional narrow groves patterned on the wire entrance and exit define electron emitter and two counters, respectively. Annealed films of AuGe constitute ohmic contacts between the 2DEG and current leads. The micromagnets are also used as side gates which, together with illumination by infrared radiation, serve for controlling the number of occupied 1D subbands.

We have applied Hall magnetometry in order to visualize directly the magnetizing process of the two micromagnets in question. Hall microbridges, patterned of GaAs/(Al,Ga)As:Si heterostructures grown in the Weizmann Institute in Rehovot, contain a 2DEG at 47.5 nm below the top surface on which Py and Co micromagnets, analogous to those in the spin-filter device, are deposited.

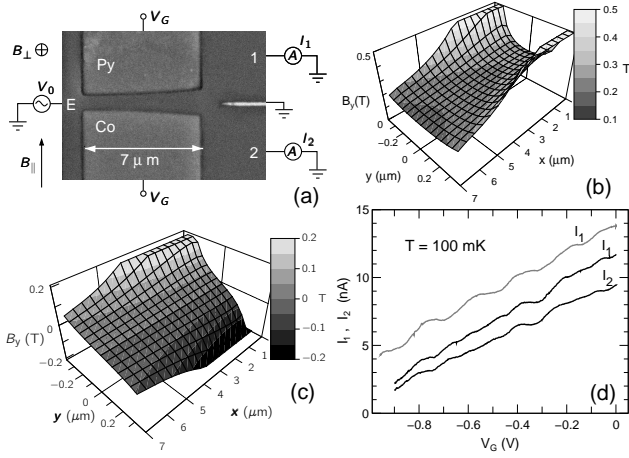


FIG. 1: (a) Scanning electron micrograph of the spin-filter device. Fixed AC voltage V_0 is applied between emitter (E) and "counters" (1), (2); DC gate voltage V_G is applied to both magnets which act as side gates. In-plane magnetizing field ($B_{||}$) and perpendicular field (B_{\perp}) are oriented as shown. (b) The in-plane magnetic field B_y (wider part of the channel is in front) calculated for half-plane, $0.1 \mu\text{m}$ thick magnetic films separated by a position dependent gap $W(x)$ and magnetized in the same directions (saturation magnetization as for Co). (c) B_y calculated for antiparallel directions of micromagnet magnetizations. (d) Counter currents I_1 and I_2 as a function of the gate voltage at $V_0 = 100 \mu\text{V}$; upper curve (shown in gray) was collected during a different thermal cycle and after longer infra-red illumination.

Figure 2 presents Hall resistance as a function of the in-plane magnetic field for three bridges which contain either single micromagnets or a pair of them. Step-like changes of the Hall resistance are caused by a consecutive reversal of magnetic domains. According to Fig. 2, the Co and Py micromagnets have differing coercive fields but similar saturation magnetizations M_s . Thus, in the spin filter device, we can compare the electric currents through the counters in the presence of the virtually uniform magnetic field (parallel magnetization directions) to the case when a strong field gradient is present. The spatial distribution of the magnetic field, evaluated under assumption that the values of M_s correspond to that of Co, $\mu_0 M_s = 0.179 \text{ T}$, are presented in Figs. 1(b) and 1(c). We see that depending on the relative magnetization directions the electrons will experience the local magnetic field B up to 0.3 T [Fig. 1(b)] or the local field gradient up to 10^6 T/m [Fig. 1(c)].

Our electron transport measurements for the spin filter device are carried out in a dilution refrigerator at 100 mK employing a standard low-frequency lock-in technique. According to results presented in Fig. 1 (d), conductance plateaux are clearly resolved. Their heights imply that the total transmission coefficient is about 0.7 , a value consistent with the presence of the reflecting barrier separating the two counters. Since during these

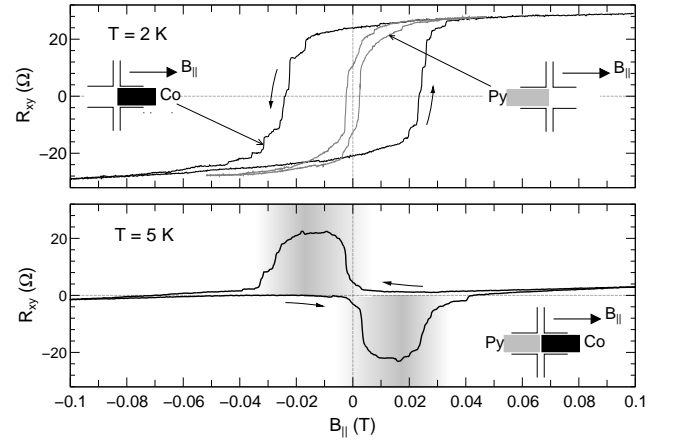


FIG. 2: Hall resistance as a function of in plane magnetic field measured for devices with single Co magnet, single Py magnet (top) and with two magnets separated by $1 \mu\text{m}$ gap (bottom). The arrows indicate directions of the magnetic field sweep. Shaded bands in lower panel denote the magnetic field range where the magnetizations of Co and Py micromagnets are antiparallel.

measurements micromagnets were not magnetized, a visible difference in counter currents provides information about the degree of structure symmetry. What should we expect when the spin-dependent potential barriers are switched on? Classically, the presence of the S-G effect should manifest itself by a gradient-induced symmetric enhancement of the current through the both counters at given emitter-counter and gate voltages. As shown in Fig. 3, we detect a current increase in both counters when a field gradient is produced by an appropriate cycle of the external magnetic field. The range of magnetic fields where the enhancement is observed corresponds to the shaded bands in Fig. 2(b). Furthermore, the magnitude of the stray field produced by Py is seen in Fig. 2(a) to diminish almost twofold prior to a change in the direction of the external magnetic field. This effect, associated with the formation of closure domains in soft magnets, explains why the current changes appear before the field reversal. The current enhancement in question is superimposed on a slowly varying background, which exhibits antisymmetric behavior for the two counters. We assign its presence to a residual effect of the Lorentz force (Hall effect) associated with a possible misalignment of the micromagnets in respect to the 2DEG plane.

We checked that results presented in Fig. 3 are unaltered by increasing the temperature up to 200 mK and independent on the magnetic field sweep rate. The relative change ΔI of counter current depends, however, on the gate voltage V_G . Figure 4 shows I_1 vs $B_{||}$ for several values of V_G (I_2 behaves in the same manner). $\Delta I/I$ increases from 0.5% at zero gate voltage to 50% close to the threshold. Furthermore, for V_G about -0.8 V ΔI is negative.

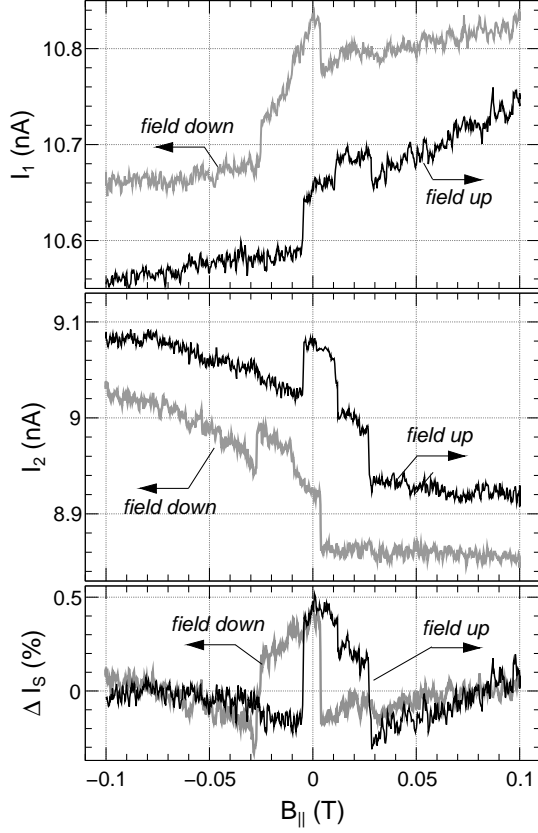


FIG. 3: Counter currents I_1 and I_2 at bias $V_0 = 100 \mu\text{V}$ and at 100 mK as a function of the in-plane magnetic field at zero gate voltage. The arrows indicate directions of the magnetic field sweep. The data for field down sweep are shifted up (by 0.05 nA) for clarity. The relative changes of symmetric component of the signal $I_S = (I_1 + I_2)/2$, which eliminates the Hall effect, are shown in the bottom panel. ΔI_S is defined as $(I_S - I_S^{++})/I_S^{++}$, where $I_S^{++} = I_S(B_{||} = 0.1 \text{ T})$.

We evaluate the expected magnitude of $\Delta I/I$ within the model of quantum ballistic transport, which we developed previously [22] by employing the recursive Green function method. We note that the key feature of our experimental configuration is a dramatic reduction of the influence of the Lorentz force by electron confinement. In particular, the effect of the in-plane magnetic field $B_{x,y}$ is much reduced by the interfacial electric field and the corresponding quantization of electron motion in the z direction. Furthermore, since a residual field B_z brought about by misalignment of the magnet centers tends to vanish in the branching region, its influence on electron dynamics will be small [23], in agreement with with a weak asymmetry of data in Figs. 3 and 4. Under these assumptions, electron dynamics is governed by the potential $V(x, y)$ determined by the device geometry, taken in the form shown in the inset to Fig. 5 as well as by the Pauli term, g^*sB , where $B = (0, B_y(x, y), 0)$ with $B_y(x, y)$ displayed in Figs. 1(b,c) for both magnetization

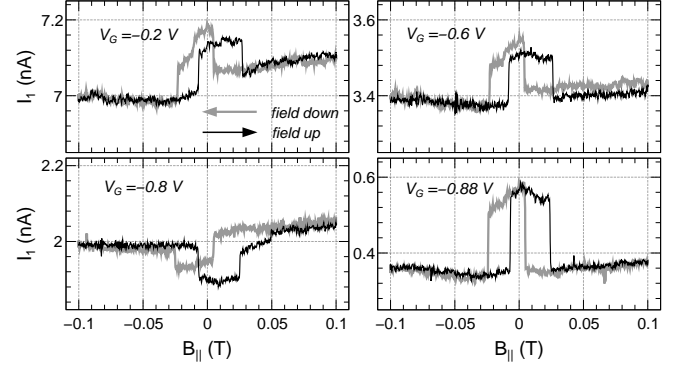


FIG. 4: The counter current I_1 as a function of the in-plane magnetic field for various gate voltages.

configurations. Because of low density of electrons in the quantum wire, we expect a considerable enhancement of the electron Landé factor. The interaction induced renormalization of the g -factor has been already observed experimentally for the gated low-density 2D electron gas [20, 21]. While the role of many body effects in confined systems is under an active debate presently, we take their existence into account by allowing for an enhancement of the Landé factor to the value $|g^*| = 2.0$.

The zero bias conductance G_0 of our model device is shown in Fig. 5(a) as a function of the electrostatic potential barrier height. Black and grey lines correspond to the Zeeman-like and Stern-Gerlach-like spin dependent barriers, respectively. As expected, when both micromagnets are polarized in the same direction an additional spin-resolved narrow *plateaux* shows up. Reversing the magnetization of Py pole while leaving the Co pole unaffected corresponds to the transition from the black to the grey curve. As a result, at the transition region between *plateaux* ΔG_0 is either positive or negative. At the quantized *plateaux*, the conductance does not depend on the type of the spin barrier, and the spatial distribution of total current density is only slightly modified by the presence of the field gradient. Under these conditions, however, the electric current at opposite edges of the device is strongly "left" or "right" spin polarized, up to 50 % for $G = 1$. This indicates that the S-G effect is present under our experimental conditions though it contributes weakly to the current enhancement visible in Figs. 3 and 4.

It is clear that ΔG should be averaged over a non-zero energy window corresponding to the applied emitter/counter voltage. Quite remarkably, the non-zero bias ($V_0 = 100 \mu\text{V}$), which is ~ 3 times larger than the expected spin splitting ($30 \mu\text{eV}$ for $g^* = 2$), does not smear out the changes of the conductance associated with the presence of the Zeeman barrier. Actually, it extends the regions of conductance changes towards the quantized *plateaux*. We defined the the observed conductance as

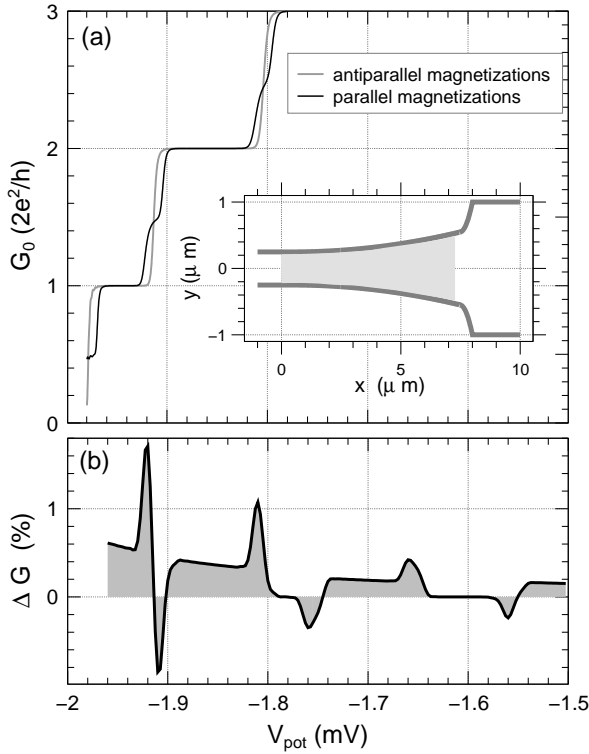


FIG. 5: (a) Quantized zero bias conductance G_0 calculated for parallel (black) and antiparallel (grey) magnetizations. The model potential $V(x,y)$ is shown in the inset. Thick dark gray line denotes the hard wall potential. Within the light grey region, an additional electrostatic potential V_{pot} is adiabatically introduced to simulate the gate potential. Conductance is shown as a function of V_{pot} for electron energy $E = 2$ meV and minimal channel width $W_0 = 0.5 \mu m$. (b) Relative changes of the conductance G for the , defined as $\Delta G = (G^{+-} - G^{++})/\langle G \rangle$, where G^{+-} corresponds to the Stern-Gerlach and G^{++} to the spin-filter configurations respectively; $\langle G \rangle$ is the average conductance for both configurations.

$G = \int_{\mu_1}^{\mu_2} G_0(E) dE$, where E is the electron energy and $\mu_2 - \mu_1 = eV_0$. We see that the computed magnitude of the effect compares favorably with the experimental findings. Except for the pinch-off region, where an additional enhancement of spin-splitting is possible, our model describes the magnitude of the effect and explains why the sign of the effect can be negative for some values of the gate voltage.

In conclusion, the experimental and theoretical study presented here demonstrates that semiconductor nanostructures of the kind proposed in this work can serve to generate and detect spin polarized currents in the ab-

sence of an external magnetic field. Moreover, according to our results, the degree and direction of spin polarization at low electron densities can easily be manipulated by gate voltage or a weak external magnetic field. While the results of our computations suggest that the spin separation and thus Stern-Gerlach effect occurs under our experimental conditions, its direct experimental observation would require incorporation of spatially resolved spin detection.

We thank H. Ohno and D. Weiss for valuable discussions. This work in Poland was partly supported by FENIKS (G5RD-CT-2001-00535) and CELDIS (ICA1-CT-2000-70018) EC projects as well as by KBN grant (PBZ-044/P03/2001).

-
- [1] D. D. Awschalom, D. Loss, N. Samarth (Eds.), *Semiconductor Spintronics and Quantum Computation* (Springer-Verlag, Berlin, 2002).
 - [2] R. M. Potok *et al.*, Phys. Rev. Lett. **89**, 266602 (2002).
 - [3] G. Grabecki *et al.*, Physica E **13**, 649 (2002).
 - [4] J. A. Folk *et al.*, Science **299**, 679 (2003).
 - [5] M. Ciorga *et al.*, Appl. Phys. Lett. **80**, 2177 (2002).
 - [6] R. Hanson *et al.*, cond-mat/0311414, unpublished.
 - [7] C. H. W. Barnes, J. M. Shilton, and A. M. Robinson, Phys. Rev. B **62**, 8410 (2000).
 - [8] M. Johnson *et al.*, Appl. Phys. Lett. **71**, 974 (1997).
 - [9] T. Matsuyama *et al.*, Phys. Rev. B **65**, 155322 (2002).
 - [10] G. Grabecki *et al.*, Physica E **21**, 451 (2004).
 - [11] N. F. Mott, Proc. Roy. Soc. London A **124**, 425 (1929).
 - [12] H. Batelaan, T. J. Gay, and J. J. Schwendimann, Phys. Rev. Lett. **79**, 4517 (1997).
 - [13] M. Garraway and S. Stenholm, Phys. Rev. A **60**, 63 (1999).
 - [14] G. A. Gallup, H. Batelaan, and T. J. Gay, Phys. Rev. Lett. **86**, 4508 (2001).
 - [15] A. Nogaret, S. J. Bending, and M. Henini, Phys. Rev. Lett. **84**, 2231 (2000).
 - [16] D. N. Lawton *et al.*, Phys. Rev. B **64**, 033312 (2001).
 - [17] S. M. Badalyan and F. M. Peeters, Phys. Rev. B **64**, 155303 (2001).
 - [18] J. Wróbel *et al.*, Phys. E **10**, 91 (2001).
 - [19] J. Fabian and S. Das Sarma, Phys. Rev. B **66**, 024436 (2001).
 - [20] J. Zhu, *et al.*, Phys. Rev. Lett. **90**, 056805 (2001).
 - [21] E. Tutuc, S. Melinte, and M. Shayegan, Phys. Rev. Lett. **88**, 036805 (2002).
 - [22] A. Łusakowski, J. Wróbel, and T. Dietl, Phys. Rev. B **68**, 081201(R) (2003).
 - [23] C. W. J. Beenaker and H. van Houten, Phys. Rev. B **63**, 1857 (1989).